Penerbit Akademia Baru

CFD Letters

Journal homepage: www.akademiabaru.com/cfdl.html
ISSN: 2180-1363

Turbulence Modelling of a Helical Savonius Wind Turbine Operating at Low Reynolds Number

Open Access

Ahmad Zakaria[1,*], Mohd Shahrul Nizam Ibrahim[1]

[1] Numerical Simulation Lab, Universiti Kuala Lumpur Malaysia Italy Design Institute, 56100 Kuala Lumpur, Wilayah Persekutuan Kuala Lumpur, Malaysia

ARTICLE INFO

Article history:
Received 19 March 2020
Received in revised form 18 May 2020
Accepted 23 May 2020
Available online 31 May 2020

ABSTRACT

Choosing a right combination of turbulence method and its associated turbulence model is important in order to ensure accuracy of CFD analysis at minimum computational cost. This is particularly true for low Reynolds number cases. In this paper, two turbulence modelling methods for predicting the performance of a helical Savonius wind turbine with 90° twist operating at Reynolds number between $6x10^4$ to $1.5x10^5$ are evaluated. The first method is Reynold-Averaged Navier-Stokes Simulation (RANS) and the other is Detached Eddy Simulation (DES). For each method, two turbulence models namely Spalart-Allmaras (SA) and Shear Stress Transport (SST) are used. The results are then compared with wind tunnel experimentation where the turbine power is computed by using the measured voltage and current relationship. RANS-SA and RANS-SST predicted a low power coefficient compared to DES-SA and DES-SST models. However, the difference between the two methods is minimal (about 3%). It is also observed that the computational time is dependent on the turbulence model. RANS-SST and DES-SST models took more than 1.5 times compared to RANS-SA and DES-SA to complete the analysis. At 5 m/s of wind speed, the power predicted by both turbulence modelling is about the same as the actual power output measured by the experiment. It can be concluded that RANS-SA model is sufficient to predict the performance of a wind turbine at a low Reynolds number. In addition, the DES method provides a detailed wake structure around and at the downstream region of the turbine. This information is beneficial in a wind farm design.

Keywords:
Turbulence model; turbulence method; RANS; DES

1. Introduction

Recent interest in Vertical Axis Wind Turbines (VAWT) type called Savonius is greatly attributed to their suitability in urban power generation applications [1,2]. Their main advantages include good starting capability and the ability to operate in any wind direction [3]. However, quite often due to its low power efficiency typically between 0.05 to 0.3 [4,5], either hybrid or incorporation of additional augmentation device have been a solution. There are also attempts to use multiple

* *Corresponding author.*
E-mail address: dzakaria@unikl.edu.my (Ahmad Zakaria)

https://doi.org/10.37934/cfdl.12.5.91100

Savonius in wind farm design as a strategy to improve overall power output [6-8]. The performance of a Savonius wind turbine usually is measured through the power coefficient (C_p), and hence current research in the Savonius rotor is always toward achieving a higher C_p.

Computational fluid dynamic (CFD) analysis is usually used to numerically predict the turbine performance regardless of actual turbine fabrication and physical testing. High fabrication cost for the physical testing is caused by the need for facilities such as wind tunnel, testing jig and complete instrumentation system [9,10]. Hence, CFD is the best alternative for physical testing with high accuracy on capturing complex flow around the Savonius wind turbine [11].

The flow around the Savonius wind turbine can be very complex as the turbine rotates at a certain rotational velocity. It has been shown that the velocity field around the Savonius wind turbine obtained by CFD analysis is quite similar to the pattern shown by particle image velocimetry (PIV) [12]. A variety of flow behavior occurred during the complete rotation of the wind turbine such as coanda like flow, dragging flow, overlap flow, stagnation flow, and vortex shedding. The flow pattern contributes to power coefficient improvement or performance reduction. The unsteady flow involved vortex shedding for isolated Savonius turbine was measured numerically and compared to published experimental data [6]. The flow pattern generated by a standalone turbine was used to estimate the consecutive turbine at the downstream position. The optimized layout makes use of the wake generated from the upstream turbine [7].

As the flow around the turbine is turbulence, the accuracy in the prediction of turbine performance is among others is dependent upon the turbulence model used in the simulation. Turbulence model selection, on the other hand, is greatly dependent on the Reynolds number, Re [13], which is

$$Re = \frac{\rho V D}{\mu} \tag{1}$$

where ρ is air density, V is wind velocity, D is turbine diameter and μ is air viscosity.

There are several standard turbulence models available in commercial CFD codes. The Spalart-Allmaras (SA) model is good for evaluating the power coefficient at a low tip-speed ratio while the k-ε model is excellent for predicting C_p at the high tip-speed ratio as found by Rogowski and Maroński, [14]. Next problem is to select the method for turbulence simulation. Direct simulation method (DNS) and Large Eddy Simulation (LES) are complex and incur a high computational cost. Due to limited computing time, the most common method is Reynold-Averaged Navier-Stokes Simulation (RANS). Detached Eddy Simulation (DES) can be considered a hybrid of RANS and LES method and yet in terms of computational cost, it is affordable using 16 core machines. The DES model is able to capture the 3D flow characteristic near the blade surface [15]. Another study by Dobrev *et.al.*, [12] used DES turbulence model to verify the PIV data of Savonius wind turbine. The combination of DES and the k-ω model shows the flow pattern approximately as generated by PIV.

While the majority of the works to date is focused on high Reynolds number i.e. at the wind speed of above 6 m/s, an analysis of low wind speed is not being reported. The main objective of this present study is to compare the performances of the two simulation methods: RANS and DES in predicting the performance of a helical Savonius rotor with 90° twist angle operating at low Reynolds number using commercial finite element based CFD code. The results are then compared with experimental data obtained from a wind tunnel test. The wake structures generated by both methods are also investigated.

2. Savonius Rotor Design

A 2D view of the Savonius wind turbine used in this study is as shown in Figure 1. The S-shaped blade has an overlap ratio of 0.242. The blade is helical with 90° twist and attached to the endplate at both ends. The height is 0.5 m and the diameter is 0.27 m resulting in an aspect ratio of 1.85. The blade is allowed to rotate in a counter-clockwise direction. The prototype model was produced using a rapid prototyping technique.

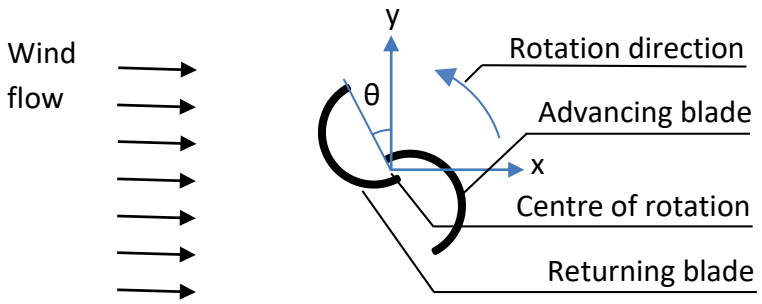

Fig. 1. 2D view of the two-bladed Savonius wind turbine

Figure 2 shows the different cross-section of 90^{o} twist Savonius wind turbine. To visualize the flow around the turbine at different rotor angle rotation, three surfaces: top, middle, and bottom were selected as denoted by sections I, II and III. The main objective is to illustrate the position of advancing blade and returning blade throughout the entire turbine revolution.

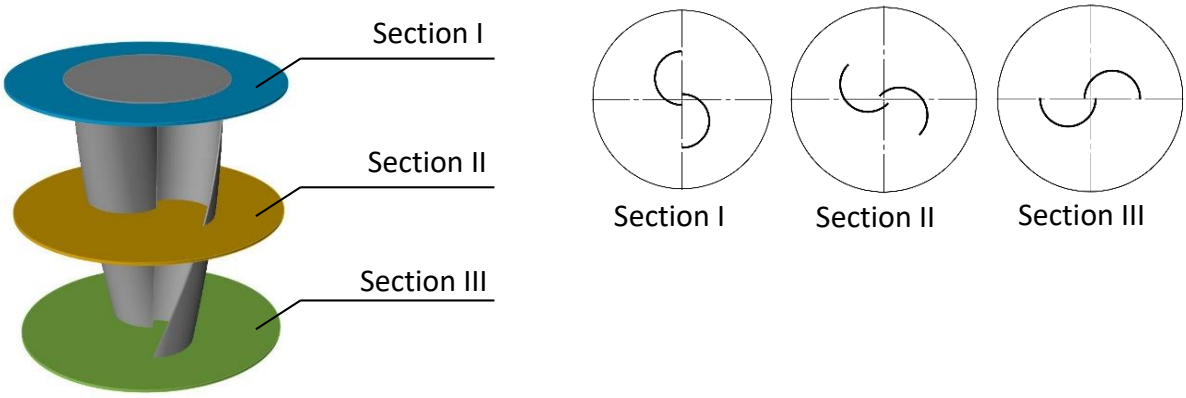

Fig. 2. 2D-view for 90^{o} twist Savonius at the different cross-section

3. CFD Method

A 3D computational domain with a dimension of 8.1 m x 4.32 m x 4.32 m used in this study. A rotating domain in the form of a cylinder with a diameter of 0.3 m and 0.55 m high defined in the computational domain and a Savonius rotor is placed in the centre of the rotating domain. The 2D view of the CFD computational domain is shown in Figure 3. Fine mesh is assigned to the rotating cylinder to enhance the ease of convergence [16]. The CFD methodology was validated by using the published wind tunnel data [17]. Figure 4 shows the grid independent study of CFD method validation [18]. The validation analysis with optimum mesh (Mesh 2) fit well the published experimental data. A layer of fine mesh is then generated across section II to capture the flow around the section. The rule of the wall for mesh creation is not implemented in order to reduce the computation time. The

transient analysis is used to capture the dynamic motion of the Savonius rotor. The widely used sliding mesh method was implemented in the present study. The rotor is allowed to rotate with assigned rotational velocity, ω [19,20] when subjected to 5 m/s wind speed. 5 revolutions of time step are set [16] with 10^o movement for every time step.

The numerical procedure was repeated for two turbulence models namely Spalart Allmaras and SST in conjunction with RANS and DES simulation methods using finite element based CFD solver Acusolve. The turbine performance was then computed based on the ratio of power generated by the rotor to the power available in the system at a wind speed of interest. The power coefficient of the turbine, C_p can be calculated based on Eq. (2).

$$C_p = \frac{\tau\omega}{0.5\rho AV^3} \tag{2}$$

where τ is average turbine torque for 5th revolution in the numerical study, ω is turbine rotational velocity at tip speed ratio, ρ is air density, A is turbine swept area and V is the wind velocity.

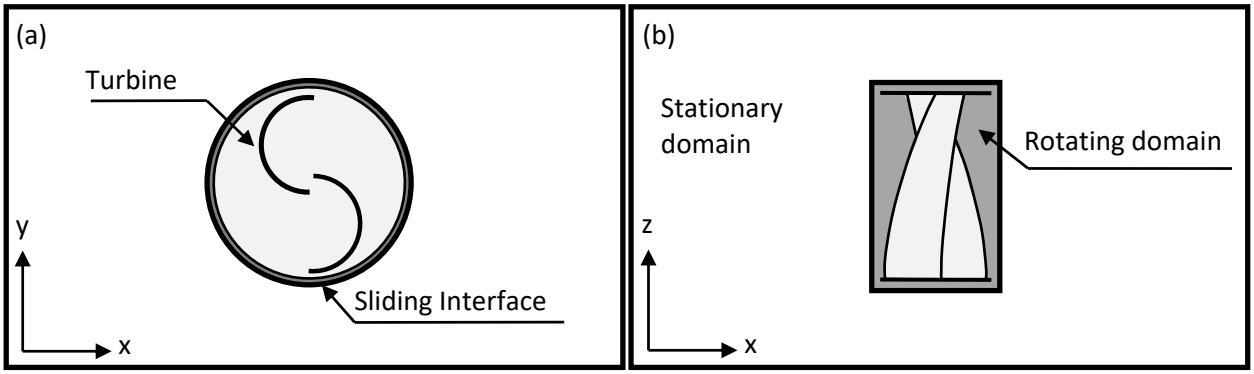

Fig. 3. CFD computational domain (a) Cross-section View (b) Side view

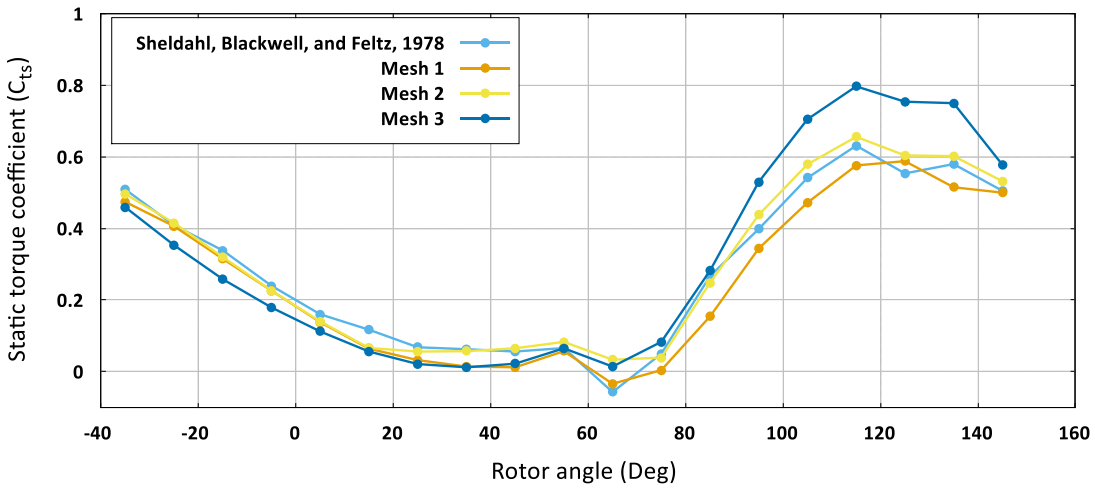

Fig. 4. Grid independence study on CFD method validation [18]

4. Wind Tunnel Experimental Procedure

The prototype turbine is directly coupled to a 12V DC coreless generator as shown in Figure 5. The whole assembly was then placed in front of an open circuit wind tunnel of 2 m x 2 m test section area. In order to monitor the output, the generator was also connected to a DC load. The generator's

output voltage and current at a wind range between 3 to 6 m/s were measured by a multimeter and the turbine rotational speed was measured by an encoder.

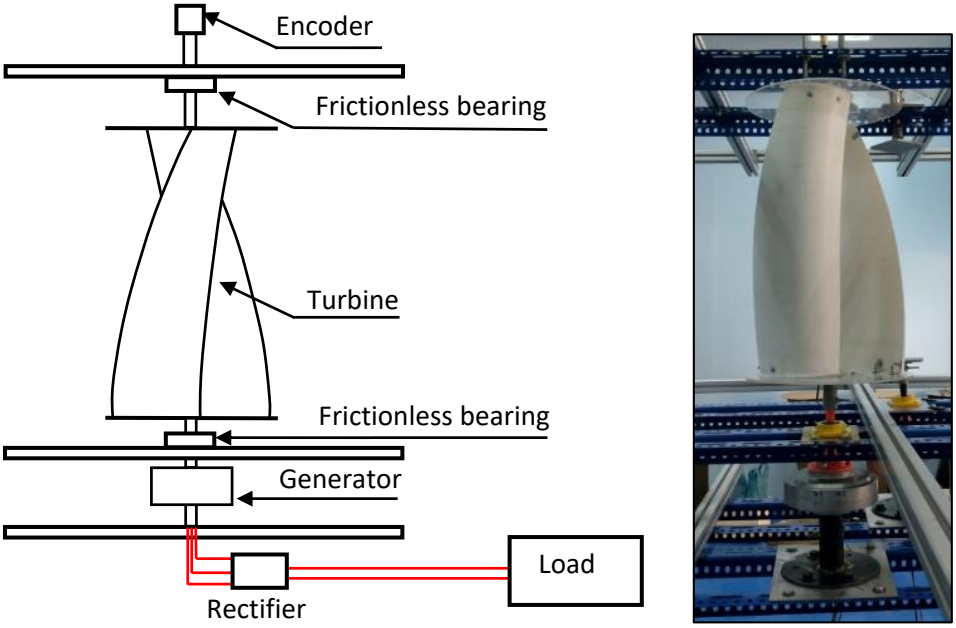

Fig. 5. Equipment setup for wind tunnel testing

The power of the turbine, P_e was computed by using Eq. (3).

$$P_e = IV \tag{3}$$

where I is generator current (A) on tested load and V is generator voltage (V) at respective wind speed. And actual torque can be obtained by Eq. (4).

$$\tau = \frac{IV}{\omega} \tag{4}$$

5. Results and Discussion

In this section, the results of different simulation methods are compared based on the computational time and accuracy of the predicted C_p with respect to the wind tunnel experiment. In addition, wakes generated are also discussed.

5.1 Numerical Prediction on Turbine Performance

Figure 6 shows the predicted C_p values for a different combination of turbulence models. The DES-based turbulence models (DES-SA and DES-SST) predicted higher values of C_p of 0.1428 and 0.1442, respectively. Whereas a lower C_p is predicted by RANS (RANS-SA, RANS-SST) simulation method. However, the difference between the lowest and the highest is small i.e. about 3%.

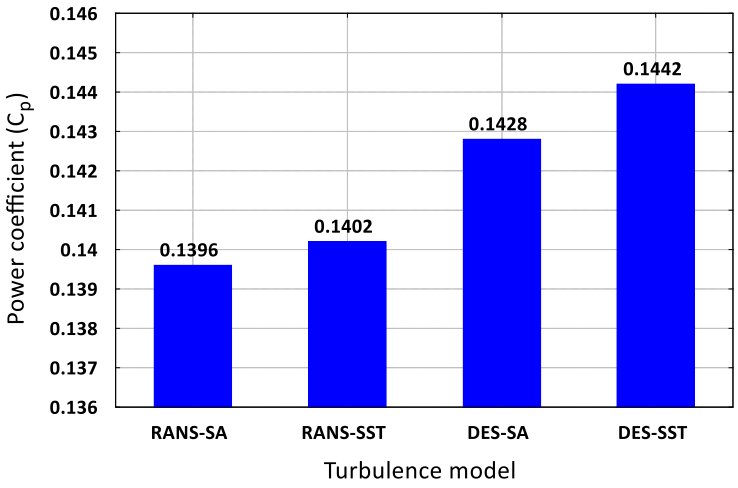

Fig. 6. Turbine performance predicted via numerical study for respective turbulence model (V=5m/s)

The computational time for the numerical study for the respective turbulence model based on a 16-core machine is shown in Table 1. RANS-SST and DES-SST require the longest computational time. Therefore, it is evident that the computational time is highly dependent on the turbulence model rather than the modelling method.

Table 1
Computational time for respective turbulence model

Turbulence model	Time (hours)
RANS-SA	6
DES-SA	7.8
RANS-SST	9.4
DES-SST	9.6

Figure 7 shows the turbine dynamic torque of the last revolution predicted by all turbulence models. They show a positive torque at all rotor angles as the blade design with a twist angle. This is a typical characteristic of a helical rotor in which the negative torque is eliminated in turbine rotation [21] giving an excellent starting capability. Again, a slightly higher torque is predicted by DES method.

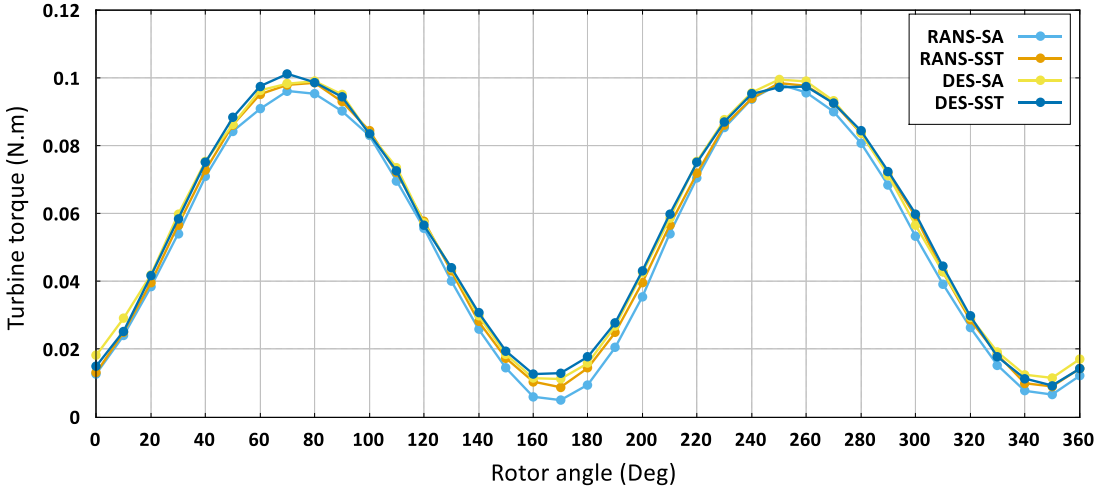

Fig. 7. Turbine torque at respective rotor angle

5.2 Flow Visualization Around the Turbine

The velocity contour for the middle section of the turbine is illustrated in Figure 8 (a-d). In general, they look the same since as the flow passes over the rotor blade, it experiences a drop in the kinetic energy and hence the speed but regains to the initial velocity at a certain distance downstream.

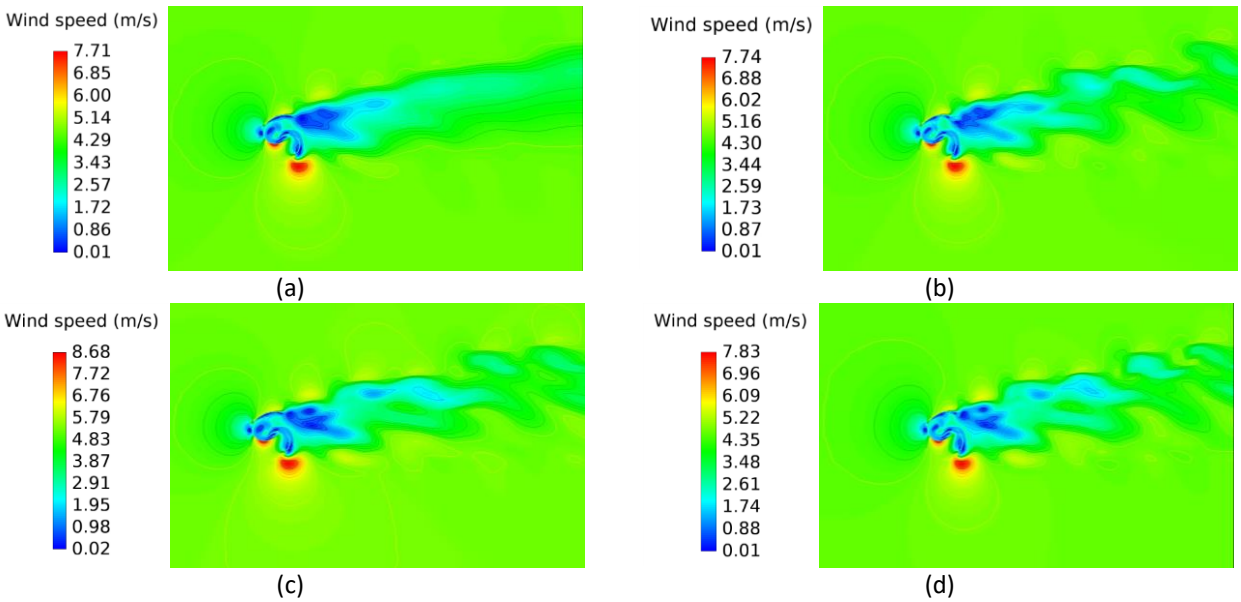

Fig. 8. CFD flow pattern for difference turbulence model prediction (a) RANS-SST, (b) DES-SST, (c) RANS-SA, and (d) DES-SA

Upon closer examination of the DES turbulence modeling, it is observed that much clearer vortices formed outside the wake especially near the blade tip and concave side of returning blade. The strong vortex formed at the returning blade is clearly captured by DES-SST turbulence model. The weak vortex region downstream of the turbine shows complex flow in both DES turbulence models. To view this flow complexity, velocity patterns for DES-SST and RANS-SST turbulence models are given in Figure 9 and Figure 10, respectively.

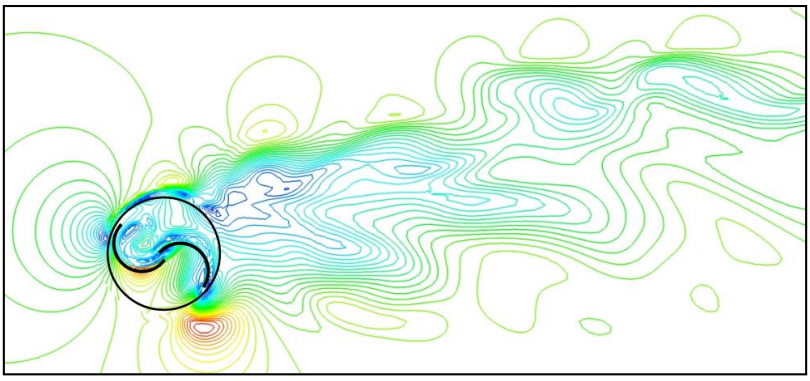

Fig. 9. Velocity contour based on DES-SST turbulence model

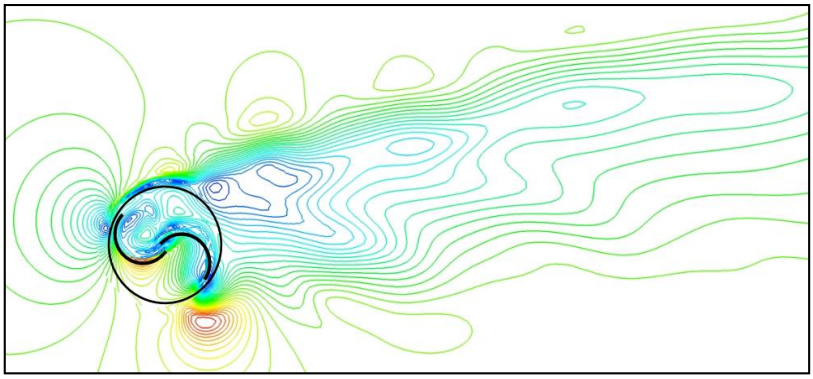

Fig. 10. Velocity contour based on RANS-SST turbulence model

The DES-based turbulence model shows a complex wake structure behind the turbine. This is especially true in the case of DES-SST where a detailed contour gradient can be observed at turbine downstream position.

The velocity contours at 0° and 30° are then compared with PIV data obtained from the previous study [12] in an attempt to verify the DES result. As shown in Figure 11, the location of the strong vortex at the advancing blade is the same for both PIV and DES model.

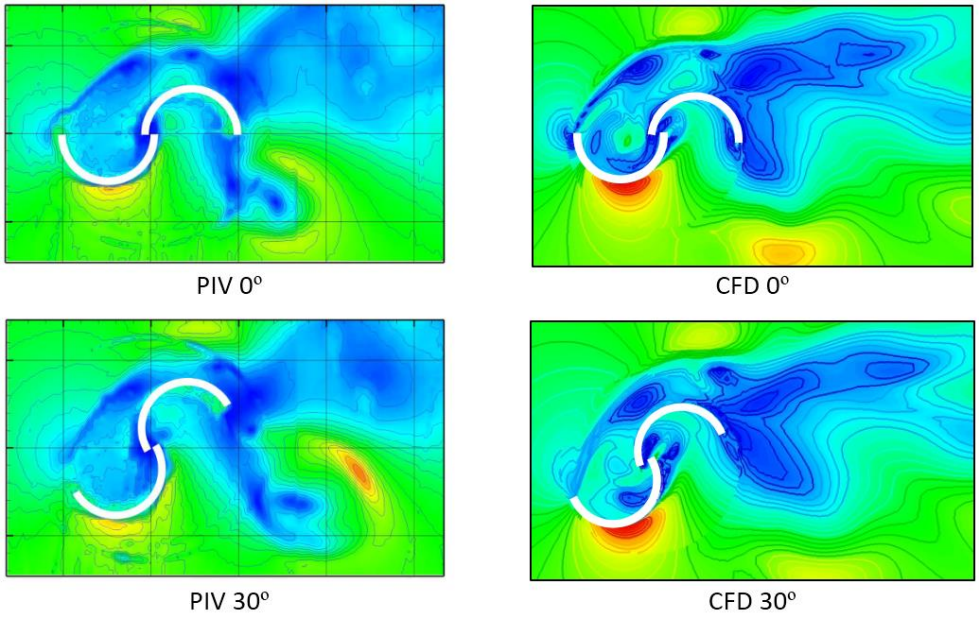

Fig. 11. Comparison between PIV data [12] and DES result

However, for the PIV velocity field, the location of the second vortex is behind the advancing blade, whereas it is on the left side of the advancing blade for the DES data. The reason for this is that a straight blade Savonius was used in the PIV method.

5.3 Wind Tunnel Experiment and CFD Validation

Figure 12 compares the actual power generated by the Savonius turbine with the values predicted by RANS-SA and DES-SA models. The actual power curve shows a gradual increase in power as the wind speed increases. On the other hand, the power predicted by the turbulence models is rather linear. This discrepancy can be explained by the sliding mesh method used in this study where the

power is computed based on the tip-speed ratio. Just like in the case of the power coefficient, the difference in the predicted power by different turbulent models is minimal.

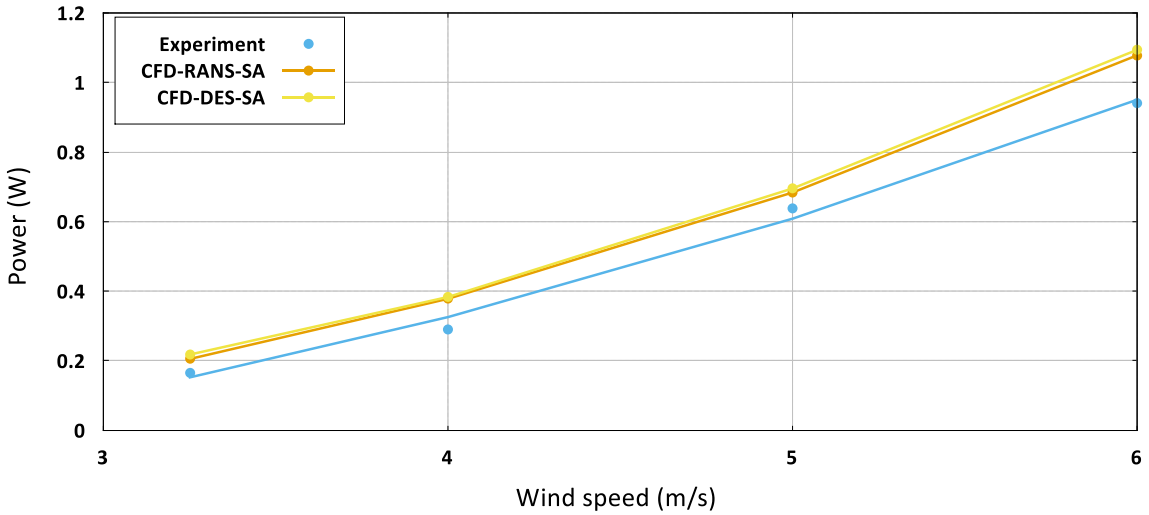

Fig. 12. Comparison between actual power and predicted power by CFD at different wind speeds

6. Conclusions

It is confirmed that RANS-SA method is sufficient to predict the performance of a wind turbine operating at low Reynolds number. In this study, the Reynolds number of interests is between $6x10^4$ to $1.5x10^5$. The computational time is found to be independent of the turbulence modelling simulation used. This is evident by the fact that the computational time for RANS-SST and DES-SST is 1.5 times longer than either DES-SA or RANS-SA. However, one main advantage of the DES approach observed in this study is that the method can provide detailed wake structure generated by the Savonius rotor. As the vortex shedding can clearly be seen at the downstream, thus making DES is more attractive for determining the right location of other turbines in a wind farm design.

Acknowledgement

The authors would like to acknowledge the Malaysian Electricity Supply Industries Trust Account (MESITA) through the Ministry of Energy, Science, Technology, Environment & Climate Change (MESTECC) for funding this research.

References

[1] Ricci, Renato, Daniele Vitali, and Sergio Montelpare. "An innovative wind–solar hybrid street light: development and early testing of a prototype." *International Journal of Low-Carbon Technologies* 10, no. 4 (2014): 420-429. https://doi.org/10.1093/ijlct/ctu016

[2] Chong, W. T., K. C. Pan, S. C. Poh, A. Fazlizan, C. S. Oon, A. Badarudin, and N. Nik-Ghazali. "Performance investigation of a power augmented vertical axis wind turbine for urban high-rise application." *Renewable Energy* 51 (2013): 388-397. https://doi.org/10.1016/j.renene.2012.09.033

[3] Altan, Burçin Deda, and Mehmet Atılgan. "A study on increasing the performance of Savonius wind rotors." *Journal of Mechanical Science and Technology* 26, no. 5 (2012): 1493-1499. https://doi.org/10.1007/s12206-012-0313-y

[4] Akwa, Joao Vicente, Horacio Antonio Vielmo, and Adriane Prisco Petry. "A review on the performance of Savonius wind turbines." *Renewable and sustainable energy reviews* 16, no. 5 (2012): 3054-3064. https://doi.org/10.1016/j.rser.2012.02.056

[5] Zemamou, M., M. Aggour, and A. Toumi. "Review of savonius wind turbine design and performance." *Energy Procedia* 141 (2017): 383-388. https://doi.org/10.1016/j.egypro.2017.11.047
[6] Shaheen, Mohammed, Mohamed El-Sayed, and Shaaban Abdallah. "Numerical study of two-bucket Savonius wind turbine cluster." *Journal of Wind Engineering and Industrial Aerodynamics* 137 (2015): 78-89. https://doi.org/10.1016/j.jweia.2014.12.002
[7] Zhang, Baoshou, Baowei Song, Zhaoyong Mao, and Wenlong Tian. "A novel wake energy reuse method to optimize the layout for Savonius-type vertical axis wind turbines." *Energy*121 (2017): 341-355. https://doi.org/10.1016/j.energy.2017.01.004
[8] Sun, Xiaojing, Daihai Luo, Diangui Huang, and Guoqing Wu. "Numerical study on coupling effects among multiple Savonius turbines." *Journal of Renewable and Sustainable Energy* 4, no. 5 (2012): 053107. https://doi.org/10.1063/1.4754438
[9] Lee, Jae-Hoon, Young-Tae Lee, and Hee-Chang Lim. "Effect of twist angle on the performance of Savonius wind turbine." *Renewable Energy* 89 (2016): 231-244. https://doi.org/10.1016/j.renene.2015.12.012
[10] Rozaim, Muhammad Faiz, Fazila Mohd Zawawi, Nur Safwati Mohd Nor, Haslinda Mohamed Kamar, and Nazri Kamsah. "Experimental study on performance of low speed wind turbine for application in Malaysia." *Journal of Advanced Research in Fluid Mechanics and Thermal Sciences* 26, no. 1 (2016): 20-28.
[11] Shahizare, Behzad, Nik Nazri Bin Nik Ghazali, Wen Chong, Seyed Tabatabaeikia, and Nima Izadyar. "Investigation of the optimal omni-direction-guide-vane design for vertical axis wind turbines based on unsteady flow CFD simulation." *Energies* 9, no. 3 (2016): 146. https://doi.org/10.3390/en9030146
[12] Dobrev, Ivan, and Fawaz Massouh. "CFD and PIV investigation of unsteady flow through Savonius wind turbine." *Energy Procedia* 6 (2011): 711-720. https://doi.org/10.1016/j.egypro.2011.05.081
[13] Aliferis, Alexander D., Marius Stette Jessen, Tania Bracchi, and R. Jason Hearst. "Performance and wake of a Savonius vertical-axis wind turbine under different incoming conditions." *Wind Energy* (2019). https://doi.org/10.1002/we.2243
[14] Rogowski, Krzysztof, and Ryszard Maroński. "CFD computation of the Savonius rotor." *Journal of Theoretical and Applied Mechanics* 53, no. 1 (2015): 37-45. https://doi.org/10.15632/jtam-pl.53.1.37
[15] Rogowski, K., Martin Otto Laver Hansen, R. Hansen, J. Piechna, and P. Lichota. "Detached Eddy Simulation Model for the DU-91-W2-250 Airfoil." In *Journal of Physics: Conference Series*, vol. 1037, no. 2, p. 022019. IOP Publishing, 2018. https://doi.org/10.1088/1742-6596/1037/2/022019
[16] Kumar, Anuj, and R. P. Saini. "Performance analysis of a single stage modified Savonius hydrokinetic turbine having twisted blades." *Renewable Energy* 113 (2017): 461-478. https://doi.org/10.1016/j.renene.2017.06.020
[17] Sheldahl, Robert E., Bennie F. Blackwell, and Louis V. Feltz. "Wind tunnel performance data for two-and three-bucket Savonius rotors." *Journal of Energy* 2, no. 3 (1978): 160-164. https://doi.org/10.2514/3.47966
[18] Zakaria, Ahmad, and M. S. N. Ibrahim. "Effect of twist angle on starting capability of a Savonius rotor–CFD analysis." *In IOP Conference Series: Materials Science and Engineering* 715, no. 1, p. 012014. https://doi.org/10.1088/1757-899X/715/1/012014
[19] Zakaria, Ahmad and M.S.N. Ibrahim. " Numerical performance evaluation of savonius rotors by flow-driven and sliding-mesh approaches." *International Journal of Advanced Trends in Computer Science and Engineering* 8, (2019): 57-61. https://doi.org/10.30534/ijatcse/2019/10812019
[20] El-Askary, W. A., Ahmed S. Saad, Ali M. AbdelSalam, and I. M. Sakr. "Investigating the performance of a twisted modified Savonius rotor." *Journal of Wind Engineering and Industrial Aerodynamics* 182 (2018): 344-355. https://doi.org/10.1016/j.jweia.2018.10.009
[21] Kamoji, M. A., S. B. Kedare, and S. V. Prabhu. "Performance tests on helical Savonius rotors." *Renewable Energy* 34, no. 3 (2009): 521-529. https://doi.org/10.1016/j.renene.2008.06.002